Energy 58 (2013) 78–85

Contents lists available at SciVerse ScienceDirect

Energy

journal homepage: www.elsevier.com/locate/energy

Model of a small steam engine for renewable domestic CHP (combined heat and power) system

G. Ferrara, G. Manfrida*, A. Pescioni

Università degli Studi di Firenze, Dipartimento di Energetica "Sergio Stecco", 50135 Firenze, Italy

ARTICLE INFO

Article history:
Received 22 August 2012
Received in revised form
13 March 2013
Accepted 14 March 2013
Available online 24 April 2013

Keywords:
Steam engine
Small combined heat and power systems
Renewable energy
Low-temperature heat sources

ABSTRACT

A small steam expander reciprocating engine is proposed for the conversion and utilization of low-grade heat resources of different nature, such as geothermal, solar, and recovery of waste heat. The engine, still to be developed for production, should be able to work with small flow rates and low upper temperature (100–150 °C), rejecting heat at a level still interesting for heating or cooling (with an absorption machine), that is, 50–80 °C. The device should be compact, simple and capable of easy control in order to match electric production and loads.

The thermodynamic model uses real-fluid and real-cycle assumptions. It includes a heat transfer model for non-adiabatic compression and expansion, losses through admission/discharge valves, and the effects of dead space. Quasi-stationary modeling of the system is applied: the results are also compared with those of a dynamic model, working under perfect-gas assumptions. The model allows to calculate and analyze the performance of the system, including its dependence on the main design parameters; it includes a preliminary design, with special reference to valve sizing. The results indicate that the proposed technical solution can be applied and that the performance of the CHP (combined heat and power) system is competitive with respect to other technologies for renewable energies.

1. Field of application of small steam engines

The concept of distributed energy conversion and utilization systems is rapidly developing, with a growing attention to off-grid concepts, allowing small houses and/or activities to be independent from services (energy, sewage, information flows) requiring expensive networks of wires and piping. Small steam engines could be devices of relevant interest for the market of combined heat and power (CHP) and distributed electricity production for dwelling applications.

Expanders considered for organic vapors in small ORC (Organic Rankine Cycle) units are usually of the scroll or screw type [1–5]; these expanders have been developed or adapted from compressors used in refrigerating units, and typically cover a range from 10 to 25 kW. The idea is to propose the development of smaller units, in the range from 1 kWe (individual dwellings, possibly connected by a smart grid) to 10 kW (covering the energy needs of small multi-family dwellings). To this end, it was decided to reconsider a well proven technology, that of reciprocating engines. The use of this machine as a steam expander can be traced back to 19th-century tradition, and design methods and technical solutions were advanced considerably in the 20th century [6]; however the technology can be revisited considering advances in materials and in engine control systems, derived from the IC engine sector. Nowadays valve opening/shutoff can be largely controlled by electronic/hydraulic systems, and for small sizes direct DC electricity production, possible at variable speed, can be proposed; it is even possible to consider adaptation of existing IC engines, or to use existing manufacturing lines for large-scale production.

1.1. Mode of operation

The reciprocating engine proposed operates with a traditional rod mechanism. The engine is placed between two reservoirs (Fig. 1): the steam vessel works as a high-pressure reservoir (HPR) and heat/steam accumulator: it is connected to the external heat source (for example, a field of solar collectors, or a geothermal heat exchanger). A recirculation loop ensures favorable conditions for heat transfer (a low quality of steam). The dry steam is taken

* Corresponding author.
E-mail addresses: Giovanni.Ferrara@unifi.it (G. Ferrara), Giampaolo.Manfrida@unifi.it (G. Manfrida).

0360-5442/$ – see front matter © 2013 Elsevier Ltd. All rights reserved.
http://dx.doi.org/10.1016/j.energy.2013.03.035

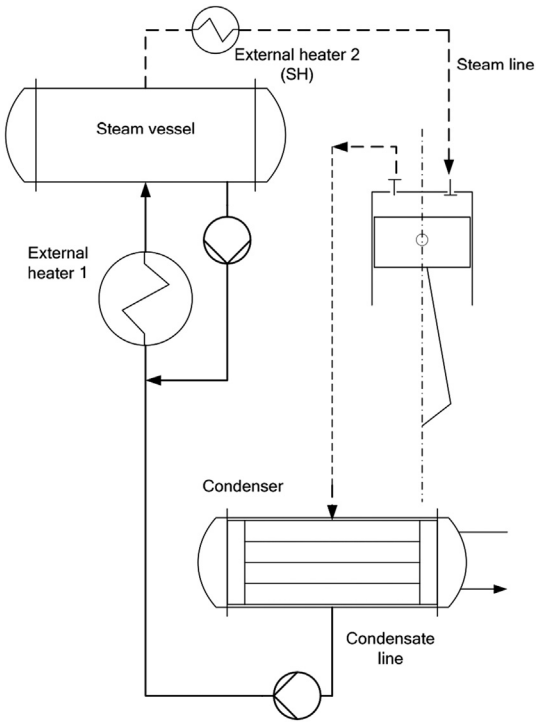

Fig. 1. Schematic of reciprocating steam engine circuit.

from the upper part of the reservoir, and routed to an external super-heater which operates directly on the engine flow rate.[1] The condenser is the low-pressure reservoir (LPR), covering the building heat load[2]: typically it is kept at a temperature of 70–90 °C.[3] A pump makes up for the pressure difference between the reservoirs.

In practice the engine would be a multi-cylinder unit, of a type similar to what has been developed for heat recovery in IC engines or for biomass applications [5,6]. With respect to a traditional cycle of an IC engine, the valve timing is completely different. A full cycle is realized in one single turn, following a two-stroke operation mode. The following description applies to the limit cycle (ideal engine, real fluid conditions), which has been previously analyzed [8]. With reference to Fig. 2, the Discharge Valve (DV) is maintained open to the Upper Dead End (UDE), so that the compression phase is absent. At the UDE, the DV is closed and the Admission Valve (AV) is opened. Steam flows under high pressure difference, rapidly filling the dead space volume (constant-volume admission, 2–5). When the HPR pressure is reached, steam flows inside the cylinder at constant pressure, with increasing volume, until the AV closes (Constant-pressure admission, 5–3). The expansion phase 3–4 is treated as adiabatic and isentropic (limit cycle). At the Bottom Dead End (BDE), the DV is opened, and steam exits the cylinder under relevant pressure difference, at constant volume (4–1); when the condenser pressure is reached, discharge of steam continues at constant pressure until reaching the upper dead end (1–2).

[1] The external Heater 2 would typically be using a heat source providing higher temperature, such as a set of parabolic trough solar collectors.

[2] During summer it is possible to consider operation of the condenser at higher temperature, and coupling to an absorption cooling loop.

[3] The condenser pressure can actually be variable, with lower values in winter (distribution of heating fuild at 60–70 °C) and higher in summer (85–95 °C, compatible with small Water/LiBr absorption machines capable of generation if cold).

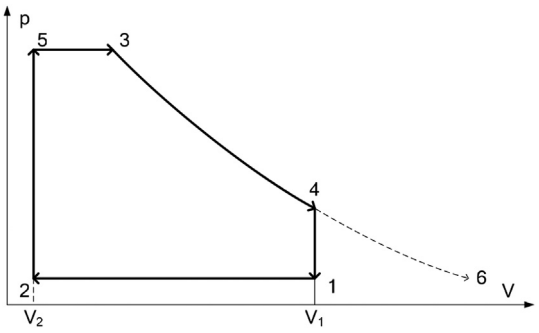

Fig. 2. Steam reciprocating engine–limit cycle.

1.2. Engine parameters

For a complete description of the cycle, the following parameters must be introduced:

Volumetric compression ratio:

$$\rho = \frac{V_1}{V_2} \tag{1}$$

Admission Grade (or Cut-Off ratio):

$$\sigma = \frac{V_3 - V_5}{V_D} \tag{2}$$

where V_D is the engine displacement, $V_D = V_1 - V_2$.

The Expansion Grade is defined as:

$$\varepsilon = \frac{V_4}{V_3} \tag{3}$$

Defining the non-dimensional dead space as:

$$\mu = \frac{V_2}{V_D} \tag{4}$$

it can be shown that:

$$\varepsilon = \frac{1+\mu}{\sigma+\mu} \tag{5}$$

The problem of determining the mass of fluid operating in the engine was thoroughly examined and the solution approach[4] was explained in Ref. [8] (considering the mass of fluid entrapped in the dead space at the end of the discharge stroke). The method is here generalized to simulation of the real cycle, considering the pressure drops in the discharge and admission valves, that is, calculating the volumetric efficiency of the engine. As in Refs. [8], no steam recompression process is considered, that is, the Discharge Valve is kept open until very close to the UDE.

2. Real cycle model

With respect to the Limit Cycle [8], the Real Cycle Model adds several complications, which result in the typical cycle diagram shown in Fig. 3, referred to a sample calculation.

Basically:

1. the base pressure at point 2 must be iterated from a first guess
2. the mass remaining in the dead space must be iterated (as in the limit case)

[4] The solution approach for determining the mass entrapped in the dead space at the UDE is similar to common practice of the limit cycle in internal combustion engines.

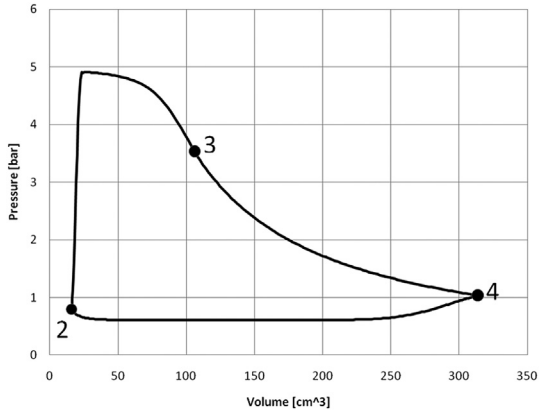

Fig. 3. Steam reciprocating engine–real cycle (Quasi-Stationary model output).

3. the admission phase is simulated with a pressure loss model, depending on the admission valve lift
4. the expansion phase includes a heat release model from the expanding fluid to the cylinder walls
5. the discharge phase is simulated with a pressure loss model, depending on the discharge valve lift.

The real cycle model requires a description of many intermediate cycle points, which are calculated from the volume-crank angle relationship:

$$V[\theta] = V_D{}^*\left[\frac{1}{\rho-1}+0.5\left(1+\frac{1}{\lambda}-\cos\theta-\frac{1}{\lambda}\sqrt{1-\lambda^2\sin^2\theta}\right)\right] \quad (6)$$

The model does not account for mechanical friction losses.

The whole model was implemented using the EES software [7], taking full advantage of the built-in steam properties which allow to consider real fluid in all thermo-fluid-dynamics processes.

2.1. Admission phase

The admission phase goes from point 2 (0° crank angle) to point 3 (beginning of expansion phase, determined by the selected Admission Grade); the fluid conditions are solved point by point with a small $d\theta$. Each point between 2 and 3 is solved with a stationary model, which consists of three steps in cascade:

a) steam enters from the AV at constant volume, passing from the HPR to the cylinder
b) steam exits from the DV, always at constant volume (only if this is kept open, DVCD > 0)
c) evaluation of the change of volume of the system (valves are still open but no steam enters or exits from the cylinder in this step). Updating of θ for next point.

The valve lift is modeled by a power law in function of θ; from the valve lift as a function of θ, the flow cross section is calculated during step a) (AV inlet flow) and b) (DV outlet flow).

During step (a), the upstream conditions are those in the HPR (superheated steam); the ideal mass flow is initially calculated using perfect-gas assumptions and isentropic flow through a convergent duct, determining if the flow is critical (as is usually at the beginning of admission, with limited lift and cross section) or subsonic. The real mass flow is calculated using the valve flow coefficient:

$$\mathrm{fc}_a = \frac{\dot{m}_r}{\dot{m}_i} = f(\mathrm{lift}, D_{\mathrm{AV}}) \quad (7)$$

The conditions inside the cylinder are updated assuming that the addition of the real mass flow through the valve takes place with an isenthalpic transformation.

During step (b) (AV, DV open), the mass flow exiting the system is calculated similarly; here, the upstream pressure is that inside the cylinder, while the downstream value is that in the LPR. Differently from step (a), the upstream condition can be of saturated steam: in this case (checked automatically by the model) it is assumed that only the gas phase contributes to the fluid dynamic action; the liquid phase contributes only to the total mass of steam inside the cylinder.

Hence, to calculate the ideal mass flow with saturated steam as upstream condition, the conditions are considered as dry saturated steam at the same temperature.

At the end of step (b) the conditions inside the cylinder are updated with the same assumption done at the end of step (a).

During steps (a) and (b) the valve lift is calculated with the following equation[5]

$$\mathrm{lift}_a = \mathrm{lift}_{a,\,\max}\left(1+\mathrm{aa}^*X^e+\mathrm{bb}^*X^f+\mathrm{cc}^*X^g+\mathrm{dd}^*X^h\right) \quad (8)$$

with

$$X = \frac{\theta-\frac{\mathrm{OD}_A}{2}}{\frac{\mathrm{OD}_A}{2}} \quad \text{or} \quad \frac{\frac{\mathrm{OD}_A}{2}-\theta}{\frac{\mathrm{OD}_A}{2}} \quad (9)$$

respectively during closure or opening of the admission valve.

During step (c) the system is treated as a closed system, solved imposing conservation of energy and mass. The crank angle θ is updated (with step $d\theta$[6]) as well as the conditions inside the cylinder; the process is then restarted from step (a) with the updated angle, until start of the expansion phase when point 3 is reached.

2.2. Expansion phase

The expansion is modeled through a step-by-step closed-system energy balance, starting at $\theta = \theta_3$:

$$u_\theta - u_{\theta-1} = -\delta \mathrm{W}_{r\theta} - \delta \mathrm{Q}_{e\theta} \quad (10)$$

At each step, $u = f(V,T) = f(\theta, T(\theta))$. The internal energy is decreasing with increasing expansion, both because of work extraction, and of heat release to the cylinder walls. This last can be evaluated as:

$$\delta \mathrm{Q}_{e\theta} = H\,S(T_{m\theta} - T_p) \quad (11)$$

The cylinder surface T_p is assumed constant; $T_{m\theta}$ is determined as the average between $T_{\theta-1}$ and T_θ (this last is unknown and determined iteratively; the isentropic value is assumed as first guess).

The expansion phase was modeled considering a sequence of at least 100 angle steps. At the end of the expansion, the overall work and heat released to the environment can be calculated summing all δWs and δQs.

2.3. Discharge phase

The discharge phase is treated similarly to the admission, from point 4 (end of expansion phase) to point 2 (0° crank angle), solved point by point as before. The three steps are:

[5] Here only the equation for the admission valve is shown. The DV is treated similarly.

[6] During the admission and discharge phases, a very small value of $d\theta$ is used, typically $d\theta = 1°$ or $0.1°$.

a) steam enters from the AV at constant volume (only if this is kept open, AVAO > 0), passing from the HPR to the cylinder
b) increase of volume of the closed system (valves are still open but no steam enters or exits from cylinder).
c) steam exits from the DV. Updating of θ. If point 2 is reached, check of convergence.

Each single step is treated as in the admission phase. When point 2 is reached, the model checks the convergence comparing the new mass with the one supposed as first guess at the beginning of the cycle. If the convergence is not acceptable (a relative error between successive iterations is used for this check), the mass of point 2 is updated as the average between the old and the new one, to start a new iterative cycle.

2.4. Model assembly–calculation of performance variables

After the detailed modeling of the admission, expansion and discharge (including overlapping of the three phases as described previously), it is possible to calculate the overall work as:

$$W_{\text{tot}} = W_{D_{\text{tot}}} + W_{A_{\text{tot}}} + W_{\text{Exp}} \tag{12}$$

where $W_{D_{\text{tot}}}$ is the Discharge work (work obtained during the Discharge Phase):

$$W_{D_{\text{tot}}} = \int_4^2 p\mathrm{d}V \tag{13}$$

$W_{A_{\text{tot}}}$ is the admission work (work obtained during the Admission Phase):

$$W_{A_{\text{tot}}} = \int_5^3 p\mathrm{d}V \tag{14}$$

and W_{Exp} is the expansion work (work obtained during expansion, with the AV and DV closed):

$$W_{\text{Exp}} = \int_3^4 p\mathrm{d}V \tag{15}$$

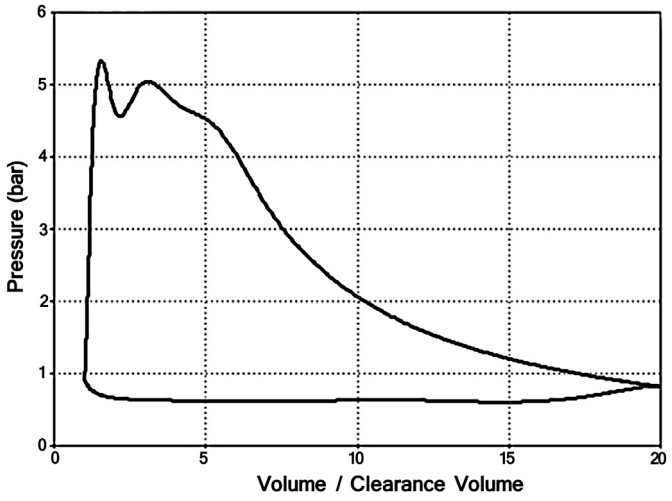

Fig. 4. Steam reciprocating engine–real cycle (Non-Stationary model output).

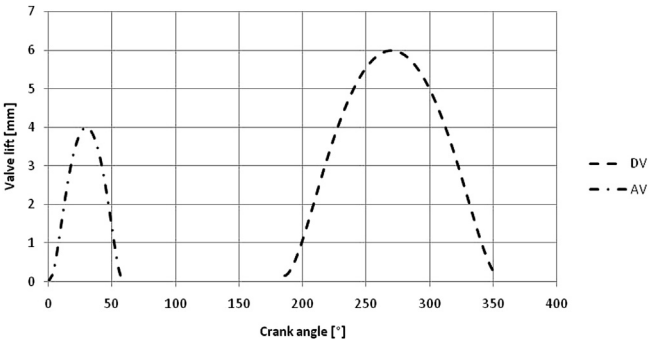

Fig. 5. Admission and discharge valve lift profiles.

The power output can be calculated as:

$$\dot{W} = \frac{W_{\text{tot}}{}^{*}\text{RPM}}{60} \tag{16}$$

The steam consumption is given by:

$$\dot{m} = (m_3 - m_2)\,{}^{*}\frac{\text{RPM}}{60} \tag{17}$$

The pump power must also be calculated when considering the cycle performance:

$$\dot{W}_{\text{Pump}} = \dot{m}^{*}(p_{\text{HPR}} - p_{\text{LPR}})/\left(\rho_{\text{LPR\_L}}{}^{*}\eta_{\text{Pump}}\right) \tag{18}$$

A value of 0.6 was assumed for the pump efficiency.
The cycle external heat input rate is:

$$\dot{Q}_{1c} = \dot{m}^{*}(h_{\text{HCR}} - h_{\text{LCR\_L}}) \tag{19}$$

Where $\rho_{\text{LPR\_L}}$ and $h_{\text{LCR\_L}}$ are calculated at pressure $p = p_{\text{LCR}}$ in liquid conditions ($x = 0$).
Using Eqs. (18) and (19), one can calculate the Cycle Efficiency as:

$$\eta_c = \frac{\left(\dot{W} - \dot{W}_{\text{Pump}}\right)}{\dot{Q}_{1c}} \tag{20}$$

As the system is conceived to provide heat and electricity for a domestic application, it is important to evaluate the exergy efficiency:

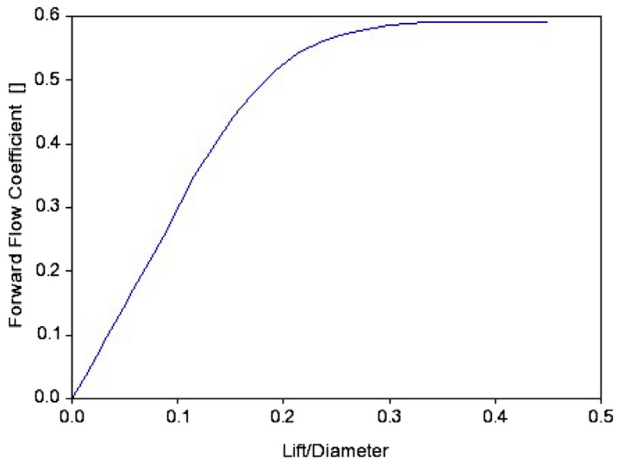

Fig. 6. Valve duct-flow coefficient.

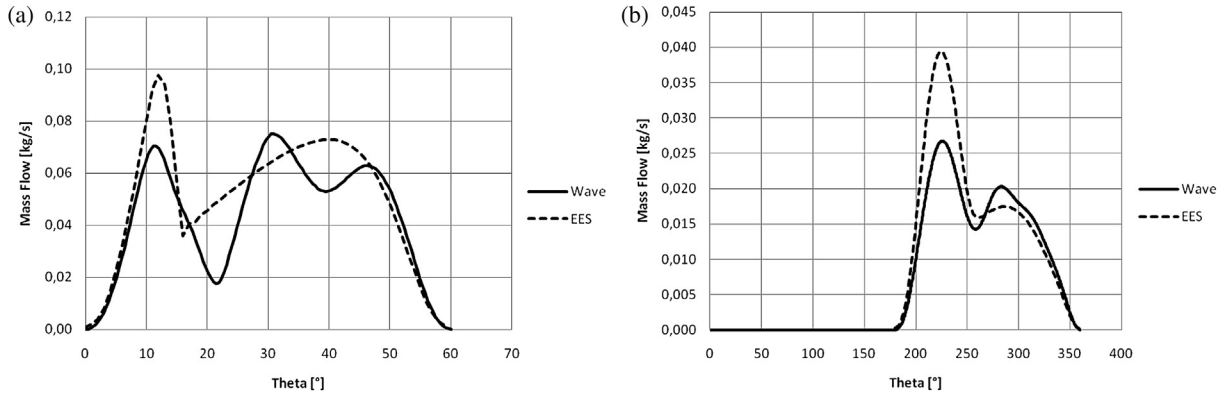

Fig. 7. Flow rate across the admission (a) or discharge (b) valve cross section; NS = solid line; QS = dotted line.

$$\eta_x = \frac{\left(\dot{W} - \dot{W}_{\mathrm{Pump}} + \dot{X}_{\mathrm{Out}}\right)}{\dot{X}_{\mathrm{In}}} \tag{21}$$

Where $\dot{X}_{\mathrm{Out}}$ and $\dot{X}_{\mathrm{In}}$ are respectively the exergy flow rates out of the condenser and that of the steam inlet stream.

2.5. Non-stationary model

The assumption of a quasi-stationary flow is often non–realistic in reciprocating engines. In the present case, the rotational speed is limited and non-stationary effects are expected negligible; however, it was decided to perform a check of the model described at point 2 using a widely-used commercial non-stationary software package developed for IC engines, WAVE [11]. Wave has not been built for such an application and so it does not allow to consider real fluids, as it applies perfect-gas relationships derived from compressible gas dynamics. However, it is fully capable to calculate wave propagation in ducts, as it solves 1-D Navier–Stokes non-stationary flow equations including, where necessary, heat transfer and pressure losses by using experimental correlations. The model was assembled following the directions of the WAVEBUILD application; a complete description of the inlet/outlet ducts geometry, valve size, lift and timing is necessary for building the model.

As a result of the calculation, a typical cycle diagram is shown in Fig. 4.

3. Reference case

As a reference case, the basic data of an experimental engine were considered [9,10].

- Volumetric compression ratio $\rho = 20$
- Displacement = 300 cm^3 (Bore × Stroke = 72.6 × 72.6 mm);
- Crank/Rod ratio = 0.27
- Discharge and Admission duct lengths = 100 mm
- Rotational speed = 2300 rpm;
- $\sigma = 0.30$ (Cut-Off, Design Value)
- AV diameter = 30 mm, maximum lift = 4 mm
- DV diameter = 30 mm, maximum lift = 6 mm

The valve lift trend vs. the crank angle θ is shown in Fig. 5. Fig. 6 shows the profile of the valve duct flow coefficient. These coefficients have been experimentally evaluated on a real engine head with a geometrical valve-duct configuration consistent with the here-presented reference case.

The operating conditions were set at values compatible with utilization of low-enthalpy heat sources, such as non-concentrating or low-concentration solar thermal collectors, or low-medium temperature geothermal resources:

- $T_{\mathrm{HPR}} = 160\ ^{\circ}\mathrm{C}$
- $P_{\mathrm{HPR}} = 5$ bar

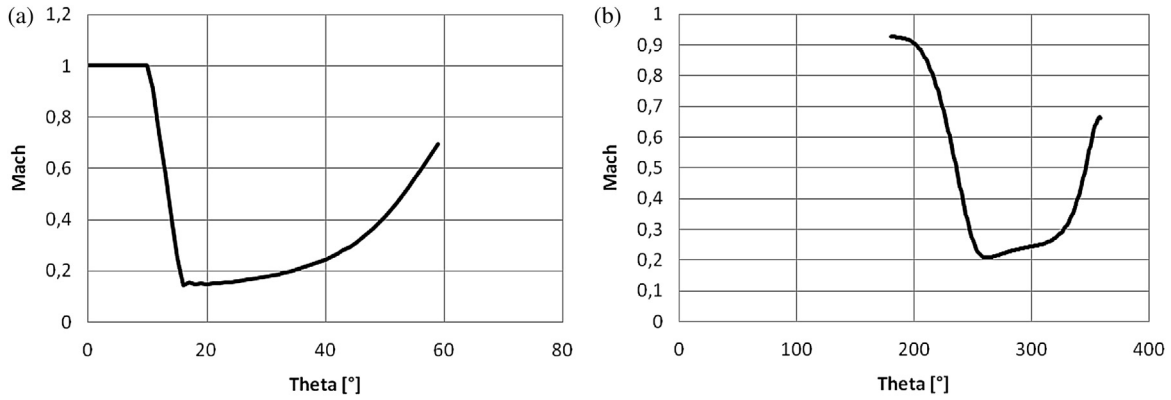

Fig. 8. Mach number across the admission (a) or discharge (b) valve cross section; (Quasi-Stationary model).

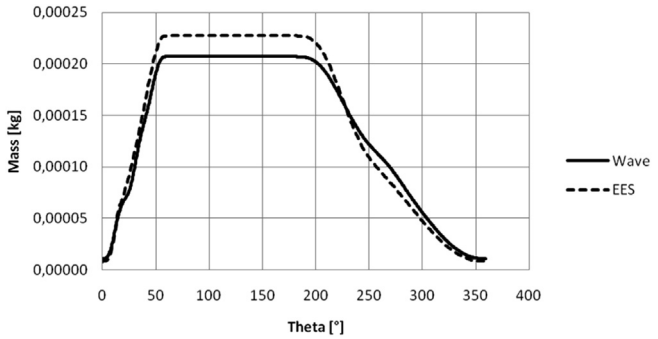

Fig. 9. Steam reciprocating engine—mass inside the cylinder; NS = solid line; QS = dotted line.

Table 1
Overall results of cycle calculations.

	QS	NS	Limit	Carnot
Cycle efficiency, %	9.3	8.7	11.1	17
Power output, kW	1.9	1.8	2.26	
Steam flow rate, g/s	8.4	7.8	10.0	
Exergy efficiency, %	87			

The LPR was kept at a temperature value compatible with a building heating system, with moderate vacuum conditions at the condenser:

- $T_{LPR} = 86\ ^{\circ}C$ (Condenser pressure $p_{LPR} = 0.6$ bar)

4. Application of the cycle models

4.1. Admission and discharge

Both models are able, through the application of Quasi-Stationary (QS) or non-stationary (NS) flow modeling equations, to calculate the flow conditions across the admission and discharge valve. As a result, the flow rates can also be calculated; these are shown for both QS and NS models in Fig. 7(a) and (b), respectively for the AV and the DV.

It can be seen that the Quasi-Stationary (QS) model is not able to reproduce the strong flow rate oscillations during the short admission phase; in the case of the DV, at least the quality of the time profile is reproduced. For the Quasi-Stationary (QS) model, which is treating real fluid (steam), it is meaningful to examine the Mach Number profiles during the admission and discharge phases, which are shown in Fig. 8(a) and (b) respectively.

As a result of the calculations of the admission and discharge processes, it is possible to calculate the mass present inside the cylinder as a function of the crank angle, which is shown in Fig. 9; it can be seen that the two models are providing similar results for this variable.

4.2. Overall performance

The overall results in terms of efficiency, power output and steam consumption are resumed in Table 1.

For comparison, the results of the limit cycle calculation [8] and the value of the efficiency of the reversible heat engine (Carnot) operating between the upper and lower temperatures is also included.

5. Parametric analyses—sensitivity to design values

After cross-validation of the two models, which was demonstrated at Section 4, it is interesting to consider their parametric application to determine:

a) Sensitivity to Cut-Off (Power modulation; Quasi-Stationary model)
b) Sensitivity to rotational speed (Partial-Load operation; Quasi-Stationary model)
c) Sensitivity to heat transfer coefficient (Expansion; Quasi-Stationary model)
d) Sensitivity to rotational speed (Partial-Load operation; Non-Stationary model)

5.1. Sensitivity to Cut-Off (power modulation; Quasi-Stationary model)

Variable Cut-Off can be an effective way of adjusting power output to the electricity load required by the local grid. The effects of changing Cut-Off on the Engine Efficiency and Power Output are shown in Fig. 10(a) and (b).

Fig. 10 shows that it is possible to increase the power output, at the expense of decreasing the engine efficiency. A Maximum Power condition is reached for very large Cut-Off values; however, the efficiency decreases too much under these extra-power conditions.

5.2. Sensitivity to rotational speed (partial-load operation; Quasi-Stationary model)

Changing the rotational speed can be an alternative to Variable Cut-Off for power modulation, if the electric generator allows

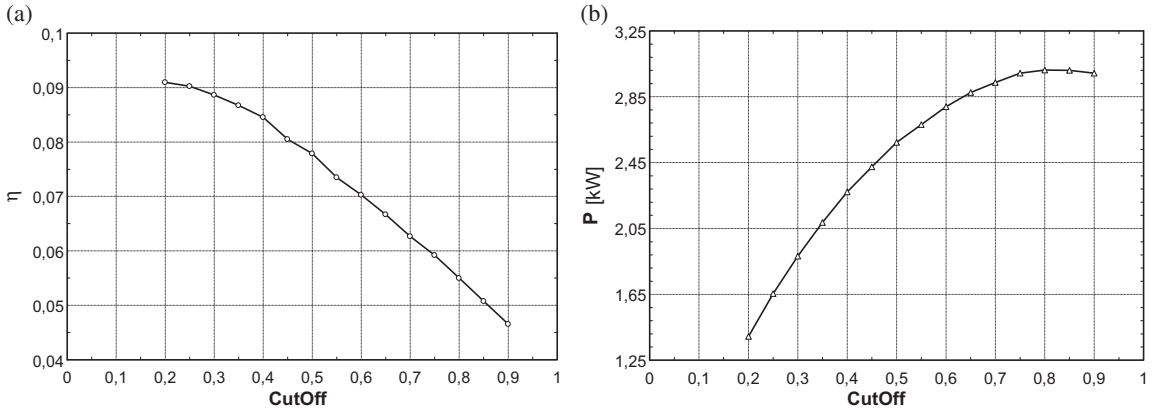

Fig. 10. Engine efficiency (a) and power output (b) with variable Cut-Off (QS model).

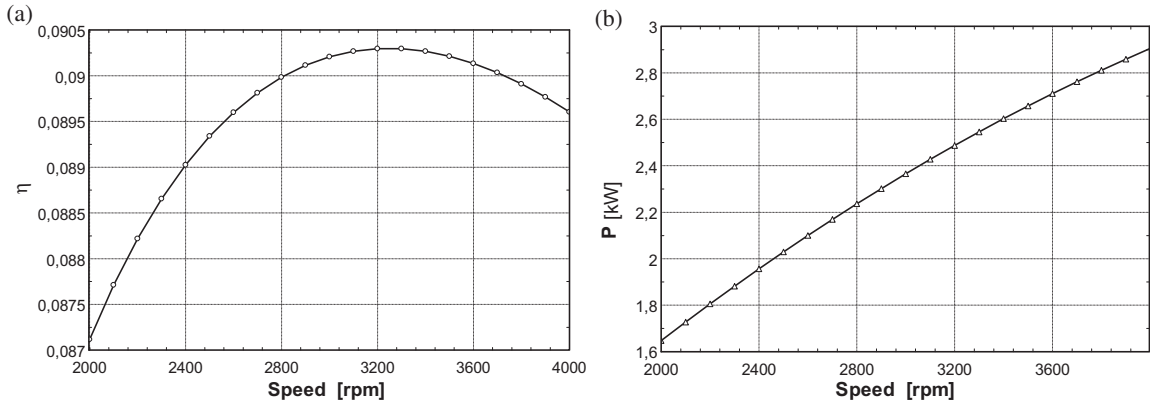

Fig. 11. Engine efficiency (a) and power output (b) with variable speed (QS model).

variable-speed operation (in practice, a DC generator with variable-speed AC inverter is needed). The effects of changing the rotational speed on the Engine Efficiency and Power Output are shown in Fig. 11(a) and (b).

Fig. 11 shows that a maximum condition for efficiency occurs at about 3200 rpm according to the model; power increases rather steadily with increasing rotational speed.

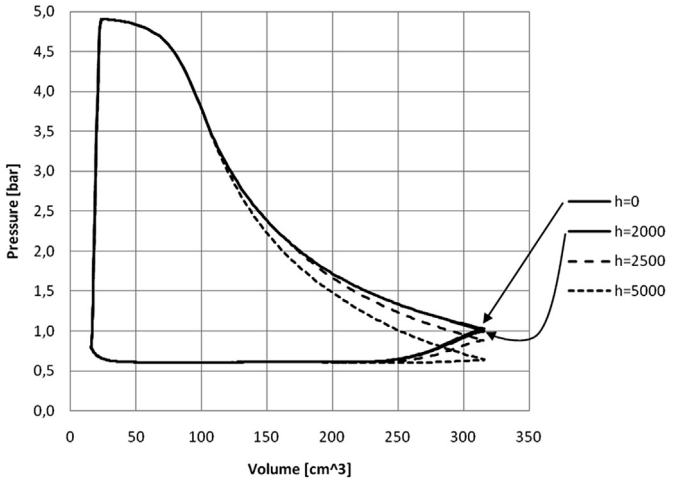

Fig. 12. Real cycle with variable H (W/(m^2°C)) (QS model).

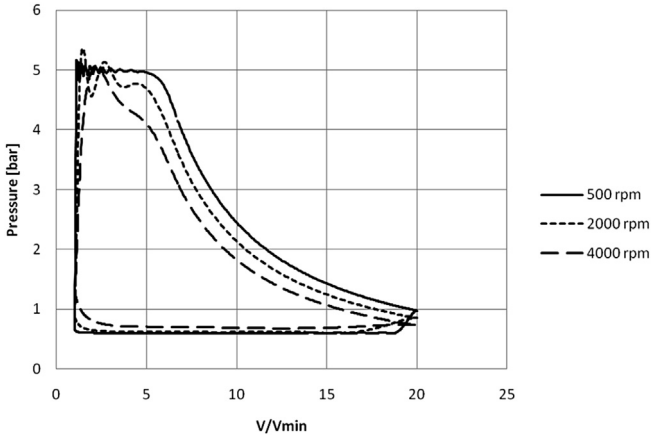

Fig. 13. Cycle diagrams calculated at variable speed (Non-Stationary model).

5.3. Sensitivity to cylinder wall heat transfer (Quasi-Stationary model)

The addition of a heat release model during the expansion represents a notable advancement from the limit to real cycle model in IC engines. This happens because the in-cylinder gas temperature can reach values which are much higher than the wall temperatures. In the present case, the real-cycle model includes wall heat transfer from the working fluid (steam) to the cylinder walls, which is modeled under the assumption of a constant overall heat transfer coefficient H. It is important to run a sensitivity analysis in order to confirm what is the influence of assuming different values of H. Fig. 12 shows cycle calculations with $0 < H < 5000$ W/(m^2°C). The conclusion is that—as expected under the assumed working conditions—the influence of heat release during the expansion is marginal for the steam reciprocating engine (Fig. 13).

5.4. Sensitivity to rotational speed (partial-load operation; non-stationary model)

Wave propagation effects can become relevant when the rotational speed is increased, with a negative effect on volumetric efficiency. In case of necessity, these problems can be cured with a careful design of the intake/exhaust system. Before this, it is important to evaluate how much the engine performance would be sensitive to operation at higher speed. Fig. 11 shows the cycle diagrams calculated by the non-stationary (NS) model for three different rotational speed values (500, 2000 and 4000 RPM). The wave oscillation pattern during the admission phase is clearly affected by rotational speed; the main effect—as expected—is a lower cycle area, which confirms the negative effect of increasing rotational speed on the engine volumetric efficiency. The effect can anyway be considered marginal, as the values of RPM should be maintained low in order to minimize problems with engine lubrication, in case that a true engine of this type should be developed.

6. Conclusions

Detailed results have been shown in Sections 4 and 5, consequently the conclusions here reported represent only a synthesis evaluation of the presented case study.

Engine models represent a precious preliminary tool before developing a true prototype: the model includes a preliminary design and sizing of the engine, and allows to calculate the expected performance; cross-validation among different models can

confirm the validity of calculations, and provide solid arguments in the direction of proposing an experimental development.

In the case of reciprocating steam engines, a Quasi-Stationary (QS) real-cycle model considering real fluid (steam) properties was developed; the model allowed simulation of a reciprocating steam engine with "traditional" (poppet) IC engine admission and discharge valve design, verifying that it was thus possible to achieve a reasonable sizing of the admission/discharge system.

A non-stationary model of the engine (NS), assuming perfect-gas fluid behavior, provided similar results confirming that unsteady flow and wave propagation effects do not alter substantially the results of the Quasi-Stationary model.

The overall performance of the engine, which is conceived for application to low-temperature heat sources (solar, geothermal) and small, distributed CHP applications (e.g., residential buildings, possibly in a smart grid arrangement) was satisfactory both from the point of view of efficiency and power output. Considering the nominal operating conditions ($T_{HPR} = 160\ ^\circ C$, $p_{HPR} = 5$ bar; $T_{LPR} = 86\ ^\circ C$, $p_{LPR} = 0.6$ bar), the cycle efficiency is about 9%, which is satisfactory compared to the Carnot (reversible engine) efficiency of 17%. From the point of view of combined heat and power, the system under nominal conditions achieves a notable value of 87% exergy efficiency.

A sensitivity analysis confirmed the possibility of using different solutions for power/load adjustment (variable cut-off or variable speed); the marginal effects of including in the model cylinder-wall heat transfer, and of the drawbacks of rotational speed on volumetric efficiency, within the expectable operating range.

Nomenclature

aa, bb, cc, dd, *e, f, g, h* parameters describing the valve lift profile
D diameter[m]
DVCD discharge valve closure delay, [°]
fc flow coefficient
h enthalpy [kJ/kg]
H heat transfer coefficient [W/(m^2 K)]
lift valve lift[m]
$\dot{m}$ mass flow rate [kg/s]
p pressure[bar]
ODA open duration of admission valve (total angle during which the valve is open)
Q heat [kJ/cycle]
$\dot{Q}$ heat rate [kW]
RPM speed of revolution [rpm]
S surface [m^2]
T temperature [°C]
u internal energy [kJ/cycle]
V volume[m^3]
W work [kJ/cycle]
$\dot{W}$ power [kW]
$\dot{X}$ exergy rate [kW]

Greek symbols
ε expansion grade
θ Crank angle
η_c cycle efficiency
λ Crank/rod length ratio
μ non-dimensional dead space
ρ volumetric compression ratio
LCR_L density of liquid at lower pressure reservoir conditions [kg/m^3]
σ admission grade (Cut-Off)

Subscripts and superscripts
a air
A admission
D discharge
d displacement
Exp expansion
HPR high-pressure reservoir
In inlet
LPR low-pressure reservoir
LPR_L low-pressure reservoir, liquid conditions
Max maximum (lift)
Out outlet
Pump pump
x exergy
1, 2, 3… points 1, 2, 3…

Acronyms
AV admission valve
AVAO admission valve advance opening
BDE bottom dead end
CHP combined heat and power
DV discharge valve
HPR high pressure reservoir
LPR low pressure reservoir
NS non-stationary model (WAVE)
ORC Organic Rankine Cycle
QS Quasi-Stationary model (EES)
UDE upper dead end

References

[1] Quoilin S, Lemort V, Lebrun J. Experimental study and modeling of an Organic Rankine Cycle using scroll expander. Applied Energy 2010;87:1260–8.
[2] Kane M, Larrain D, Favrat D, Allani Y. Small hybrid solar power system. Energy 2003;28:1427–43.
[3] Kim HJ, Ahn JM, Park I, Rha PC. Scroll expander for power generation from a low-grade steam source. Proceedings of the Institution of Mechanical Engineers, Part A: Journal of Power and Energy 2007;221(5):705–12.
[4] Smith IK, Stosic N, Aldis CA. Development of the trilateral flash cycle system part 3: the design of high efficiency two-phase screw expanders. Proceedings of the Institution of Mechanical Engineers, Part A: Journal of Power and Energy 1996;210(A2):75–93.
[5] Badr O, Naik S, O'Callaghan PW, Probert SD. Expansion machine for a low power-output steam Rankine-cycle engine. Applied Energy 1991;39:93–116.
[6] Acton O, Caputo C. Compressori ed espansori Volumetrici. UTET; 1992.
[7] http://www.fchart.com/ees/; 2013.
[8] Manfrida G, Marraccini L. Model of a steam/organic vapour volumetric reciprocating expander. In: Proceedings of ECOS 2010, Lausanne. 2010.
[9] Badami M, Mura M. Design and performance evaluation of an innovative small scale combined cycle cogeneration system. Energy 2008;33:1264–76.
[10] Badami M, Mura M. Preliminary design and controlling strategies of a small-scale wood waste Rankine Cycle (RC) with a reciprocating steam engine (SE). Energy 2009;34:1315–24.
[11] http://www.ricardo.com/en-GB/What-we-do/Software/Products/WAVE/; 2013.